

This is the accepted manuscript made available via CHORUS. The article has been published as:

Accurate measurement of the first excited nuclear state in ^{235}U

F. Ponce, E. Swanberg, J. Burke, R. Henderson, and S. Friedrich

Phys. Rev. C **97**, 054310 — Published 10 May 2018

DOI: [10.1103/PhysRevC.97.054310](https://doi.org/10.1103/PhysRevC.97.054310)

Accurate Measurement of the First Excited Nuclear State in U-235

F. Ponce, E. Swanberg, J. Burke, R. Henderson, S. Friedrich

Lawrence Livermore National Laboratory, 7000 East Ave., Livermore, CA 94550

We have used superconducting high-resolution radiation detectors to measure the energy level of metastable ^{235m}U as 76.737 ± 0.018 eV. The ^{235m}U isomer is created from the alpha decay of ^{239}Pu and embedded directly into the detector. When the ^{235m}U subsequently decays, the energy is fully contained within the detector and independent of the decay mode or the chemical state of the uranium. The detector is calibrated using an energy comb from a pulsed UV laser. A comparable measurement of the metastable ^{229m}Th nucleus would enable a laser search for the exact transition energy in $^{229}\text{Th} - ^{229m}\text{Th}$ as a step towards developing the first ever nuclear (baryonic) clock.

The desire to develop nuclear clocks with a potential accuracy of one part in 10^{19} is currently driving the interest in low-energy metastable nuclear states [1, 2]. Nuclear clocks could exceed the accuracy of atomic clocks by several orders of magnitude, because the long lifetimes of metastable nuclear states translate into narrow intrinsic linewidths, and because small nuclear dimensions make energy levels less susceptible to Zeeman and Stark shifts. The increased accuracy would e.g. enable new tests of fundamental physical constants [3], advanced geodesy [4], and novel approaches to detect dark matter [5] and gravitational waves [6].

^{229}Th has the lowest-energy excited state known at 7.8 ± 0.5 eV [7]. This makes it the primary isotope of interest for nuclear clocks because the energy of the excited state is accessible with tunable laser sources. However, the accuracy of this measurement [7] is not sufficient to justify a laser search for the exact transition energy since the excited state is extremely narrow and the photon absorption cross section is extremely small. Several experiments have attempted to measure the energy of ^{229m}Th directly and with high accuracy [8–10], but either showed no signal [11, 12] or were compromised by secondary effects [13–16]. The first unequivocal direct

detection of a metastable state in ^{229}Th has recently confirmed that the lowest-energy excited state has a life time above one minute if the Th ion is at least doubly charged so that the decay by internal conversion is suppressed [17]. In solids, the decay of $^{229\text{m}}\text{Th}$ by internal conversion is possible and the life time is reduced to 7 μs [18]. However, a high-accuracy measurement of the $^{229\text{m}}\text{Th}$ transition energy is still missing. Here we describe a new technique to measure the energy of low-energy metastable states with an accuracy of a few tens of meV. We demonstrate this approach with a very accurate measurement of $^{235\text{m}}\text{U}$, the second-lowest known nuclear excited state at 76.5 ± 0.4 eV [19-21]. Finally, we discuss how this experiment can be adapted to measure the decay energy of $^{229\text{m}}\text{Th}$ with similar accuracy.

$^{235\text{m}}\text{U}$ has a half-life of ~ 26 minutes, necessitating its continuous production for our experiment. A 7200 Bq ^{239}Pu source electroplated onto aluminized mylar alpha decays into $^{235\text{m}}\text{U}$ with a branching ratio of 98% [21]. The plutonium is only ~ 10 nm thick to allow recoiling $^{235\text{m}}\text{U}$ nuclei to escape and be embedded in the detector. The aluminized mylar is sufficiently thin to transmit the 355 nm light of the calibration laser (Fig. 1). The ^{239}Pu source is mounted ~ 3 mm from the detector. A micromachined Si collimator prevents decay products from striking the detector substrate. The detectors are superconducting tunnel junctions (STJs) with Ta-Al electrodes on both sides of an Al_2O_3 tunnel barrier, fabricated at STAR Cryoelectronics LLC [22]. They exploit the small ~ 0.7 meV energy gap in superconducting Ta so that photon or particle absorption excites $\sim 1000\times$ more signal charges than in typical semiconductor detectors, with the expected factor of ~ 30 improvement in energy resolution [23, 24]. In addition, STJ detectors do not have a dead layer, so that events from particles absorbed near the surface will not suffer any signal loss. For our experiments, we use two Ta(300nm)-Al(50nm)- Al_2O_3 (2nm)-Al(50nm)-Ta(165nm) STJs with an area of $(138 \mu\text{m})^2$ on a single Si chip. They have an energy resolution of ~ 2 eV FWHM in the EUV range, rise times of $\sim 8 \mu\text{s}$, and decay times of tens of μs [25]. The ^{239}Pu source and STJ detectors are cooled to ~ 100 mK in an adiabatic demagnetization refrigerator (ADR). The detectors are operated in a magnetic field of 15 mT to suppress the dc Josephson current and voltage biased at 100 μV . Signals are amplified with a current-sensitive preamplifier optimized for STJ operation and processed with a trapezoidal filter with a 10 μs rise time [26].

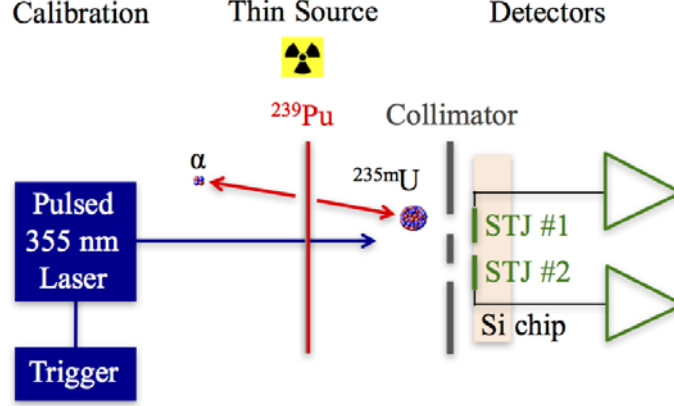


Figure 1: Schematic of experimental setup: $^{235\text{m}}\text{U}$ recoil ions produced by the decay of ^{239}Pu are embedded in the STJ detectors, which measure their subsequent decay into the ^{235}U ground state.

The detector response is continuously calibrated with a pulsed frequency-tripled Nd:YVO₄ laser (Spectra Physics, model J40-B16-106Q) that is fed into the cryostat through an optical fiber. The laser is triggered at a rate of 100 pulses per second. Each laser pulse deposits an integer number of photons in the STJ detector, so that the calibration spectrum consists of a comb of evenly spaced peaks that correspond to different numbers of absorbed photons. The laser wavelength has been measured accurately in air at ambient temperature with a UV grating spectrometer (Thorlabs CCS150), which in turn was calibrated using the line emission from a Hg vapor lamp at the same time under the same conditions [27]. We determine a laser wavelength of 354.377 ± 0.016 nm in air, corresponding to an energy of 3.49865 ± 0.00015 eV per photon. The measured wavelength is slightly shorter than the literature value of 354.71 ± 0.01 nm [28], which according to the manufacturer is not unexpected for this laser after years of use. We have confirmed that the laser wavelength does not change for different excitation currents due to heating. For STJ calibration, the laser intensity is adjusted so that the laser energy comb distribution is roughly centered around the expected energy of the $^{235\text{m}}\text{U}$ decay.

$^{235\text{m}}\text{U}$ recoil nuclei that escape from the Pu source have a maximum energy of 84 keV and are embedded in the STJ detectors up to a maximum depth of ~ 10 nm. This is comparable to the absorption length of ~ 12 nm for 3.5 eV photons in Ta. Since photon and electron energies relax over length scales of hundreds of nm inside the detector, we expect no systematic error due

a potential depth dependence of the responsivity. In contrast, ^{239}Pu alpha particles will traverse the STJ detector and stop in the Si substrate. The exposure to high-energy ions in a magnetic field can cause magnetic flux trapping and thus alter the leakage current and gain of the STJ detector. The detector response therefore shows small irregular drifts over the ~ 20 hours data acquisition of a single ADR cycle. This drift is corrected by a continuous energy calibration using the laser energy comb. All data are recorded in list mode, and the energy calibration is performed over 5-minute intervals. The calibration spectra are measured in coincidence with the trigger signal of the laser, while the $^{235\text{m}}\text{U}$ signal is measured in anti-coincidence. Each 5-minute calibration spectrum is fitted to a superposition of multiple Gaussian functions using ROOT [29], with the fit restricted to peaks with more than 800 counts. Spectra are subsequently re-binned with a bin width of 0.2 eV. For 5-minute intervals, central peaks in the region of interest contain roughly 6000 counts, and their centroids can thus be determined with a statistical precision of ~ 10 meV rms. Sum spectra for a single day contain roughly a million counts per peak and have a statistical precision below 1 meV. Since the Gaussian fits of the outermost peaks of the laser energy comb are unreliable, their centroids are not included in the linear energy calibration of the STJ response. Different choices of the time interval for partitioning the data change the calibration by no more than 2 meV at the energy of $^{235\text{m}}\text{U}$.

During laser calibration, we observe an offset that scales linearly with the average number of photons in the spectrum. This offset is due to the unavoidable absorption of laser photons in the Si substrate of the STJ detector chip whose energy is transferred to the STJ by the athermal phonons produced during their relaxation. They create additional signal charges in the STJ and thus cause an offset in the calibration spectra that scales linearly with the laser intensity [30]. This offset is not present in the nuclear signals, which are measured in anti-coincidence with a laser pulse. We therefore determine the responsivity of the STJ from the spacing of neighboring laser peaks and set the offset to zero. The uncertainty in this offset contributes a systematic error of ± 10 meV that dominates the calibration accuracy. This energy calibration places the weak carbon K fluorescence that is observed for data acquisition times above a few days at 278.3 ± 0.8 eV and the oxygen K fluorescence at 523.8 ± 0.6 eV, which is consistent with the literature values of 277 ± 2 and 524.9 ± 0.7 eV, respectively [31].

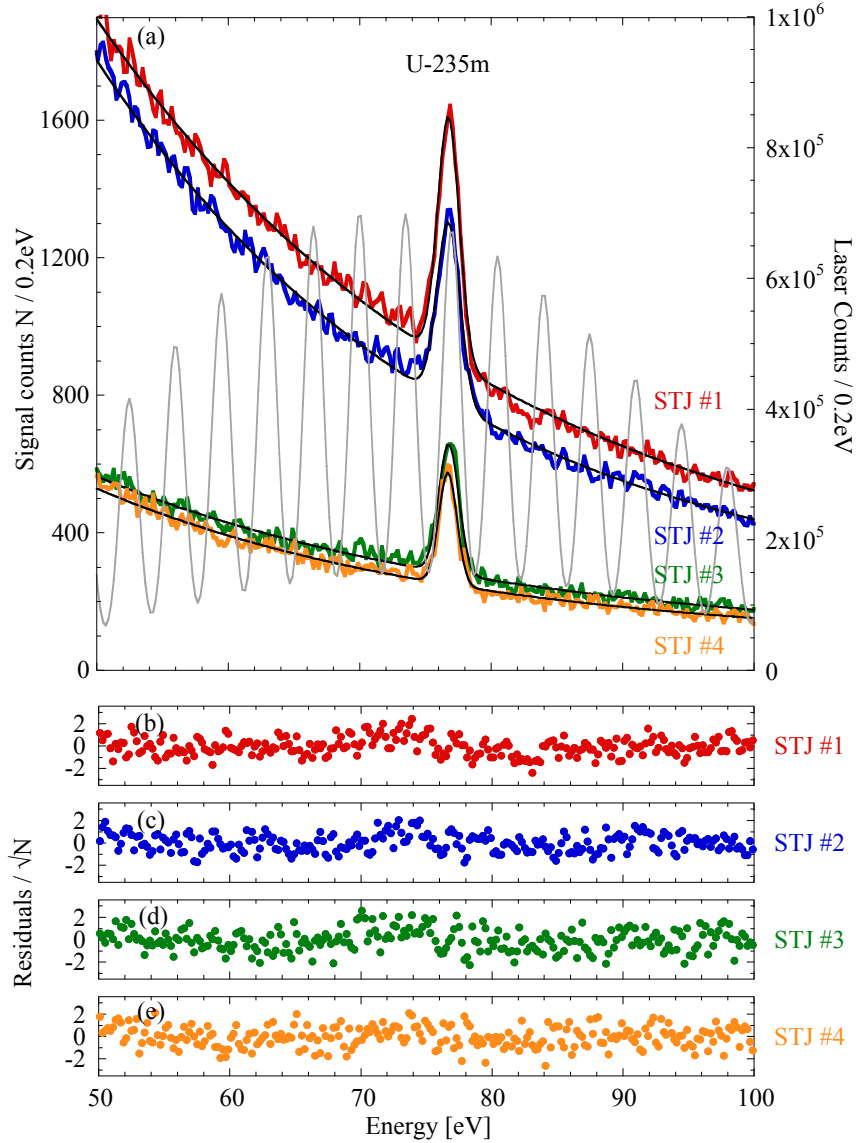


Figure 2 (a): Sum spectra from the four STJ detectors with Gaussian fits on an exponential background. The laser calibration signal, shown in grey for only one of the detectors, is measured in coincidence with the trigger, the signal from the nuclear source in anti-coincidence. (b)-(e): The normalized residuals show the overall quality of the fits, with a hint of preferentially positive residuals just below the energy of $^{235\text{m}}\text{U}$.

Figure 2 shows the summed signals with their fits and a calibration spectrum for a data acquisition time of 21 days for STJ #1 and #2 and 7 days for STJ #3 and #4, respectively. The decay of $^{235\text{m}}\text{U}$ produces a single peak above the background at a rate of ~ 1 count/minute, and no

other peaks due to partial absorption of the energy are observed. The peak shape is Gaussian, and its width of 1.9 ± 0.1 eV FWHM agrees with the widths of the calibration peaks with similar energy. The only deviation from a Gaussian response is a hint of slightly positive residuals in the energy range just below the $^{235\text{m}}\text{U}$ signal. It may indicate a change in chemical state during nuclear de-excitation or an energy loss to the desorption of surface molecules during the subsequent energy relaxation for a small fraction of the $^{235\text{m}}\text{U}$ decays. But the effect, if real, is too small to affect the value of the $^{235\text{m}}\text{U}$ energy. Since the exact shape of the spectral background around the $^{235\text{m}}\text{U}$ peak is not known, the choice of the function to approximate this background and the choice of the fit range introduce a systematic uncertainty in the analysis. To assess its magnitude, we approximate the background by different functions over different energy ranges around the $^{235\text{m}}\text{U}$ peak and determine the fluctuations in the centroid value using ROOT. For a background approximated by a quadratic, a single exponential, or a sum of two exponentials, the goodness of fit is nearly identical, and the $^{235\text{m}}\text{U}$ centroids differ by less than 6 meV. A linear or an inverse ($1/E$) background do not match the data for fit ranges >20 eV and are excluded from the analysis. Table 1 summarizes the statistical and systematic energy uncertainties of the $^{235\text{m}}\text{U}$ state.

Source of Uncertainty	Magnitude
Total statistical uncertainty	13 meV
Laser energy	4 meV
Calibration accuracy	10 meV
Choice of time interval	2 meV
Background approximation	6 meV
Total systematic uncertainty	13 meV
Total uncertainty	18 meV

Table 1: Uncertainty budget

To confirm these numbers, we have repeated the measurement with two different $(138 \text{ }\mu\text{m})^2$ STJ detectors on a new chip from the same wafer. The results of the four individual STJ measurements of the $^{235\text{m}}\text{U}$ energy are $76.739 \pm 0.022_{\text{stat}}$, $76.741 \pm 0.028_{\text{stat}}$, $76.758 \pm 0.024_{\text{stat}}$ and $76.694 \pm 0.025_{\text{stat}}$ eV (Figure 2). The results are consistent, and the centroids have a standard

error of ± 14 meV in agreement with the calculated uncertainties (Table 1). When fitting a Gaussian to the sum of the four spectra in ROOT, the centroid is given by $76.737 \pm 0.013_{\text{stat}}$ eV. Adding the systematic and statistical uncertainties in quadrature, we obtain a value of 76.737 ± 0.018 eV for the energy of metastable $^{235\text{m}}\text{U}$.

This measurement of the energy of $^{235\text{m}}\text{U}$ is an order of magnitude more precise than the current literature value, which has an uncertainty of 0.4 eV [21]. The current method is less susceptible to systematic errors, because the $^{235\text{m}}\text{U}$ nucleus is embedded in the detector so that the total energy of the isomer decay is captured independent of the decay mode and the chemical state of the uranium. Interestingly, the energy we extract is within the uncertainty quoted for the previous measurements, which relied on electron spectroscopy of the conversion electrons and could therefore have been affected by the chemical state of the uranium and by electron energy loss during escape from the sample [19, 20]. Our measurement confirms that the $^{235\text{m}}\text{U}$ in the earlier measurements had, as claimed, likely been present as $^{235\text{m}}\text{UF}_4$, i.e. in the same chemical state as the reference sample used for calibration.

This technique could be extended to measure the energy of $^{229\text{m}}\text{Th}$ with some modification, required because the lifetime of $^{229\text{m}}\text{Th}$ in solids is only 7 ± 1 μs [18]. This is comparable to the rise time and much shorter than the ~ 50 μs signal fall time of our STJ detectors, so that the detector response to a $^{229\text{m}}\text{Th}$ recoil ion will not have fallen to zero at the time of the $^{229\text{m}}\text{Th}$ decay into the ground state, especially if the recoil ion carries a kinetic energy of many keV. The recoil ions therefore need to be slowed down before they are embedded into the STJ. This can be done in high-purity He gas, since the $^{229\text{m}}\text{Th}$ life time in its ionized state exceeds 1 minute [17]. The cold ions can then be directed into the STJ detector with a well-controlled kinetic energy of ~ 10 eV. The subsequent spectrum will show two peaks, one at the kinetic plus ionization energy of the ^{229}Th ion for the nucleus in its ground state, and one with higher energy due to the $^{229\text{m}}\text{Th}$ decay. The branching ratio for $^{229\text{m}}\text{Th}$ sets the magnitude of the second peak at 2% of the primary peak, and the energy difference between the peaks is given by the decay of the $^{229\text{m}}\text{Th}$ into the ground state, which will occur during the STJ signal rise and simply add to the measured signal amplitude.

In summary, we have measured the energy of the first excited nuclear state in ^{235}U as 76.737 ± 0.018 eV by embedding $^{235\text{m}}\text{U}$ inside a superconducting tunnel junction detector and

observing its decay into the ground state. The experiment minimizes systematic errors due to chemical effects on the electron binding energies of uranium, and detector calibration with a pulsed UV laser ensures a precise energy scale. The approach can be adapted to measure the decay of metastable $^{229\text{m}}\text{Th}$ as a step towards developing a nuclear clock with unprecedented accuracy.

This work was performed under the auspices of the U.S. Department of Energy by Lawrence Livermore National Laboratory under Contract DE-AC52-07NA27344. It was funded by the LLNL LDRD Grant 14-LW-073 and by U.S. DOE Grants DE-SC0004359 and DE-SC0006214.

References

1. E. Peik, C. Tamm, *Europhys. Lett.* **61**, 181 (2003)
2. C. J. Campbell, A. G. Radnaev, A. Kuzmich, V. A. Dzuba, V. V. Flambaum, A. Derevianko, *Phys. Rev. Lett.* **108**, 120802 (2012)
3. W. G. Rellergert, D. DeMille, R. R. Greco, M. P. Hehlen, J. R. Torgerson, E. R. Hudson, *Phys. Rev. Lett.* **104**, 200802 (2010)
4. M. Bondarescu, R. Bondarescu, P. Jetzer, A. Lundgren, *Eur. Phys. J. Web Conf.* **95**, 04009 (2015)
5. A. Derevianko, M. Pospelov, *Nat. Phys.* **10**, 993 (2014)
6. S. Kolkowitz, I. Pikovski, N. Langellier, M. D. Lukin, R. L. Walsworth, J. Ye, *Phys. Rev. D* **94**, 124043 (2016)
7. B. R. Beck, J. A. Becker, P. Beiersdorfer, G. V. Brown, K. J. Moody, J. B. Wilhelmy, F. S. Porter, C. A. Kilbourne, R. L. Kelley, *Phys. Rev. Lett.* **98**, 142501 (2007); and B. R. Beck et al., LLNL-PROC-415170 (Lawrence Livermore National Laboratory, 2009)
8. G. M. Irwin, K. H. Kim, *Phys. Rev. Lett.* **79**, 990 (1997)

9. D. S. Richardson, D. M. Benton, D. E. Evans, J. A. R. Griffith, G. Tungate, Phys. Rev. Lett. **80**, 3206 (1998)
10. X. Zhao, Y. N. Martinez de Escobar, R. Rundberg, E. M. Bond, A. Moody, D. J. Vieira, Phys. Rev. Lett. **109**, 160801 (2012)
11. E. Browne, E. B. Norman, R. D. Canaan, D. C. Glasgow, J. M. Keller, J. P. Young, Phys. Rev. C **64**, 014311 (2001)
12. J. Jeet, C. Schneider, S. T. Sullivan, W. G. Rellergert, S. Mirzadeh, A. Cassanho, H. P. Jenssen, E. V. Tkalya, E. R. Hudson, Phys. Rev. Lett. **114**, 253001 (2015)
13. R. W. Shaw, J. P. Young, S. P. Cooper, O. F. Webb, Phys. Rev. Lett. **82**, 1109 (1999)
14. J. P. Young, R. W. Shaw, O. F. Webb, Inorg. Chem. **38**, 5192 (1999)
15. S. B. Utter, P. Beiersdorfer, A. Barnes, R. W. Lougheed, J. R. Crespo López-Urrutia, J. A. Becker, M. S. Weiss, Phys. Rev. Lett. **82**, 505 (1999)
16. E. Peik, K. Zimmermann, Phys. Rev. Lett. **111**, 018901 (2013)
17. L. von der Wense, B. Seiferle, M. Laatiaoui, J. B. Neumayr, H.-J. Maier, H.-F. Wirth, C. Mokry, J. Runke, K. Eberhardt, C. E. Dußmann, N. G. Trautmann, P. G. Thirolf, Nature **533**, 47 (2016)
18. B. Seiferle, L. von der Wense, P. G. Thirolf, Phys. Rev. Lett. **118**, 042501 (2017)
19. V. I. Zhudov, A. G. Zelenov, V. M. Kulakov, V. I. Mostovoi, B. V. Odinov, JETP Lett. **30**, 516 (1979)
20. A. D. Panov – Program and Thesis, Proc. 46th Ann. Conf. Nucl. Spectrosc. Struct. At. Nuclei, Moscow, p.340 (1996)
21. E. Browne, J. K. Tuli, Nucl. Data Sheets **122**, 205 (2014); the value of 76.0(4) eV on page 221 of this paper is a typographic error introduced in 2014 when re-evaluating the nuclear data (E. Browne, private communication)
22. M. H. Carpenter, S. Friedrich, J. A. Hall, J. Harris, W. K. Warburton, R. Cantor, IEEE Trans. Appl. Superconductivity **23**, 2400504 (2013)

23. S. Kraft, P. Verhoeve, A. Peacock, N. Rando, D. J. Goldie, R. Hart, D. Glowacka, F. Scholze, G. Ulm, J. Appl. Phys. **86**, 7189 (1999)
24. K. Segall, C. Wilson, L. Frunzio, L. Li, S. Friedrich, M. C. Gaidis, D. E. Prober, A. E. Szymkowiak, S. H. Moseley, Appl. Phys. Lett. **76**, 3998 (2000)
25. F. Ponce, M. H. Carpenter, R. Cantor, S. Friedrich, J. Low Temp. Phys. **184**, 694 (2016)
26. W. K. Warburton, J. T. Harris, S. Friedrich, Nucl. Inst. Meth. A **784**, 236 (2015)
27. C. J. Sansonetti, M. L. Salit, J. Reader, Appl. Opt. **35**, 74 (1996)
28. X. Délen, F. Balembois, P. Georges, J. Opt. Soc. Am. B **28**, 972 (2011)
29. R. Brun, F. Rademakers, Nucl. Inst. Meth. A **389**, 81 (1997)
30. C. M. Wilson, L. Frunzio, D. E. Prober, IEEE Trans. Appl. Superconductivity **13**, 1120 (2003)
31. J. A. Bearden, A. F. Burr, Rev. Mod. Phys. **39**, 125 (1967)